Colloid Polym Sci (2006) 284: 449–454
DOI 10.1007/s00396-005-1401-7

SHORT COMMUNICATION

Limei Wang
Dajun Chen

A one-pot approach to the preparation of silver-PMMA "shell-core" nanocomposite

Received: 12 May 2005
Accepted: 24 August 2005
Published online: 15 October 2005

L. Wang · D. Chen (✉)
State Key Lab for Modification of Chemical Fibers and Polymer Materials, College of Materials Science and Engineering, Donghua University, Shanghai 200051, China
E-mail: cdj@dhu.edu.cn

Abstract In the present work, we describe a "one-pot" route for the preparation of silver-PMMA nanocomposite. The formation of silver-PMMA nanocomposite takes into consideration the fact that free radical species are generated from the redox system containing $AgNO_3$, H_2O, and $NaBH_4$. The methyl methacrylate (MMA) monomer is at first emulsified by OP-10 to form micelle. The mercaptoethanol plays an important role in the process of forming silver-PMMA shell-core structure. Polymerization of MMA takes place when the Ag^+ is reduced to Ag. The free radical polymerization mechanism has been proposed according to the result of ESR analysis. The structure of the silver-PMMA nanocomposite has been characterized by FTIR, XRD, TEM, AFM, and DLS measurements.

Keywords Silver-PMMA nanocomposite · Shell-core · One-pot · Free radical · Redox

Introduction

Nanotechnology is currently witnessing impressive advances in aspects such as synthesis of nanoparticles, understanding their fundamental physical and chemical properties, and organization of nanoscale matter using weak, noncovalent interactions [1, 2]. Nanosized metal and semiconductor particles possess unique electronic, optical, and catalytic properties that are obviously different from bulk macrocrystallites [3, 4]. In particular, fabrication of metal-coated latex core-shell particles is currently an attractive area of investigation because of their applications in the fields of surface-enhanced Raman scattering (SERS), catalysis, or potential uses in optoelectronicdevice, in ultrasensitive chemical and biological sensor etc. [5–9].

Many researches have reported supports coated with noble metal colloids. These include platinum nanoparticles coated on polystyrene microspheres [10]. Oldenburg et al. reported on a colloid reduction chemical route for the formation of solid-core/gold nanoshell particles [11]. The deposition of silver nanoparticles on silica spheres was carried out using an inverse micelle method [12], nonionic reverse micelles [13], pretreatment steps in electroless plating [14], the sol-gel method [15], and the layer-by-layer technique [16]. However, in most cases, a general strategy based on a two-step process involving the synthesis of supports and subsequent "shell" growth has been proposed. These approaches required complicated apparatus and complex process control.

In an earlier report, we have briefly introduced a new strategy for the preparation of silver-polymer composite nanospheres with core-shell structure [17]. The proposed approach has two essential features: (1) "one-pot" route for preparation of nanocomposite in situ by chemical reduction and (2) the nanocomposite is successfully synthesized without typical initiation. Compared with previous methods of preparing nanocomposite, the route presented here is simpler and more effective, which may stimulate technological interests. In the present work, we have further investigated the mechanism of polymerization by electron spin resonance (ESR) analysis. The structure and morphology of the silver-PMMA

nanocomposite have been characterized by Fourier transform infrared spectrometer spectrophotometer (FTIR), X-ray diffraction (XRD), Transmission electron microscopy (TEM), Atomic force microscopy (AFM), and Dynamic light scattering (DLS) measurements.

Experimental section

Materials

All reagents like $AgNO_3$, $NaBH_4$, CH_3CH_2SH and methyl methacrylate (MMA) were analytic reagents and all the aqueous solutions were prepared using triply distilled water. Polyoxyethylene octylphenolether (OP-10), the emulsifier, was a commercial product and was used as received.

Preparation procedure

The preparation procedure of the Ag-PMMA nanocomposite was as follows: One gram of OP-10 was dissolved in 20 ml of distilled water at room temperature by magnetic stirring. Then 4 ml of MMA was dropped into the solution under stirring for a few minutes to form an emulsion. Two microliters of 0.01 mol/L CH_3CH_2SH in ethanol was added dropwise to the emulsion under stirring for about an hour. Then 30 ml of freshly prepared 0.004 M $AgNO_3$ aqueous solution was added to the emulsion under stirring. To the resulting emulsion, 30 ml of freshly prepared 0.4 mol/L $NaBH_4$ aqueous solution was added all at once.

Measurements

The ESR spectra were recorded by an ER 200D—SRC type spectrometer with 100 KHz modulation frequency at room temperature. The freshly prepared sample was put into the ESR tube, then 20 μL of 100 mmol/L 5,5-dimethyl-1-pyrroline N-oxide (DMPO) was added. The microwave power level was kept at 20 W and the modulation amplitude was kept at 2 G during the experiment. The infrared spectra were recorded by Nicolet Impact NEXUS-670 FTIR. The sample was ground with dried potassium bromide (KBr) powder and compressed into a disc, and then was subjected to analysis. Powder XRD pattern was obtained by employing a Rigaku D/Max-B X-ray diffractometer(100 kV, 200 mA) with Cu-K_α radiation (ł = 0.1542 nm). TEM measurement was performed on a Hitachi H-800 instrument operated at an accelerating voltage of 100 kV. Samples for TEM analysis were prepared by placing a drop of the silver-polymer nanocomposites thin solution onto a carbon-coated TEM copper grid. AFM was performed with a Multimode NanoScope IV. Tapping mode was employed in air at the cantilever's resonant frequency using a probe and cantilever unit composed of silicon. The particle size and particle-size distribution were measured by DLS with Zetasizer Nano-Series of Malvern instruments at room temperature.

Results

Structure characterization

Figure 1 shows the FTIR spectra of standard amorphous PMMA and the silver-PMMA nanocomposite. It can be seen that the characteristic absorption peaks of PMMA at ca. 2,950, 1,730, 1,460, and 1,150 cm^{-1} are clearly seen in the silver-PMMA nanocomposite. All these characteristic peaks are quite similar to that of PMMA. Figure 2 shows the XRD pattern of silver-PMMA nanocomposite. It can be seen that the XRD pattern shows diffraction peaks at 2θ of ca. 38.2°, 44.6°, 64.1°, and 77.5°, respectively. For PMMA is a typical amorphous polymer, the diffraction peaks in the XRD pattern should be ascribed to the crystal structure of silver. According to the results of reference [18], these peaks are corresponding to the 111, 200, 220, and 311 planes of the silver nano-crystals with cubic symmetry.

Morphology observations

Figure 3a and b is the TEM images of the silver-PMMA nanocomposite. As can be seen from Fig. 3, the average size of the particles is about 70 nm in diameter.

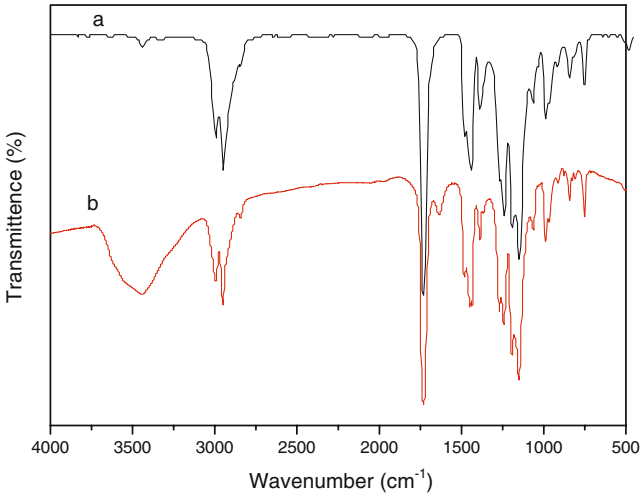

Fig. 1 Fourier transform infrared spectrometer spectrophotometer (FTIR) spectra of samples **a** the standard amorphous PMMA; **b** the silver-PMMA nanocomposite

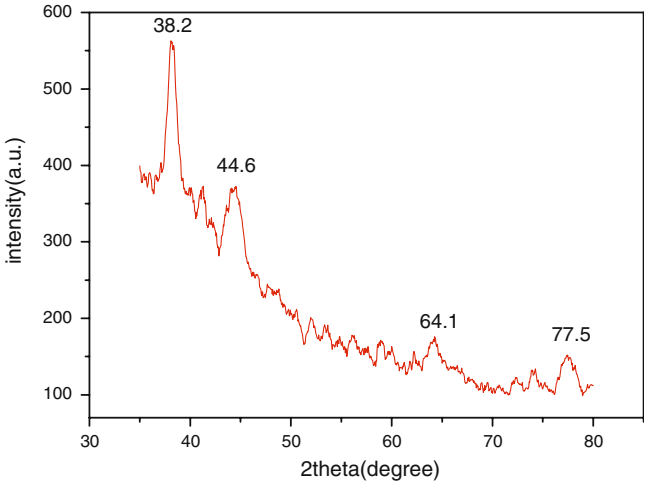

Fig. 2 X-ray diffraction (XRD) pattern of the silver-PMMA nanocomposite

The contrast between the dark edge and the misty center of the particles exhibits its core-shell structure with the shell thickness of ca. 10 nm. The electronic density of silver is much larger than that of PMMA, therefore, the dark edge of the particles is ascribed to the silver shell. Furthermore, AFM was used to study the surface morphology of the as-prepared sample. The phase image of the silver-PMMA nanocomposite is shown in Fig. 4. It can be seen that the surface morphology of the particles is a sphere with the diameter of ca. 90 nm, which is quite consistent with the result of TEM observation.

To record the phase image, the phase lag of the cantilever vibration compared to the z-piezo drive voltage was monitored with the probe scanning the surface with a preset constant amplitude of vibration. The phase data contain additional information about the tip-sample interactions resulting from adhesion, surface stiffness, and viscoelastic effects [19]. It can be seen from Fig. 4 that the dark and bright regions in the AFM image clearly define the two phase structure of the particles.

Discussion

A proposed mechanism of the fabrication procedure

According to the above results, the silver-PMMA nanocomposite with core-shell in nature was prepared. Chen and co-workers have reported the one-pot synthesis of polystyrene nanospheres with silver colloids on their surfaces by the initiator of polymerisation 2,2-azobisisobutyronitrile (AIBN) [20]. In our method, polymer nanospheres with silver colloids on their surfaces were prepared by the one-pot route without typical initiation. The formation process of the sample is illustrated in Scheme 1. The MMA monomer is at first emulsified by OP-10 to form micelle. The mercaptoethanol plays an important role in the process of forming silver-PMMA shell-core structure. It functions as the surface of the monomer droplet, which favors forming Ag-S covalent bond [18]. The mechanism of the formation of Ag-polymer nanocomposites takes into consideration the fact that free radical species are generated from the redox system containing $AgNO_3$, H_2O, and $NaBH_4$. When Ag^+ is reduced to Ag nanoparticle, the surface of the silver nanoparticle remains highly active. It adsorbs hydrogen-free radicals occurred from excessively BH_4^- ions, which stabilizes the hydrogen-free radicals throughout the course of the polymerization.

In order to investigate the polymerization mechanism of MMA in the formation process, ESR measurement

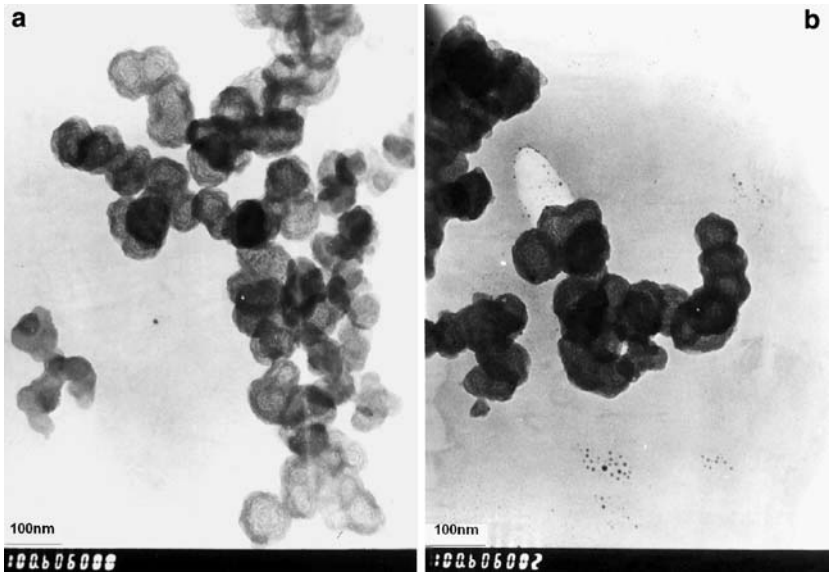

Fig. 3 Transmission electron microscopy (TEM) image of the silver-PMMA nanocomposite

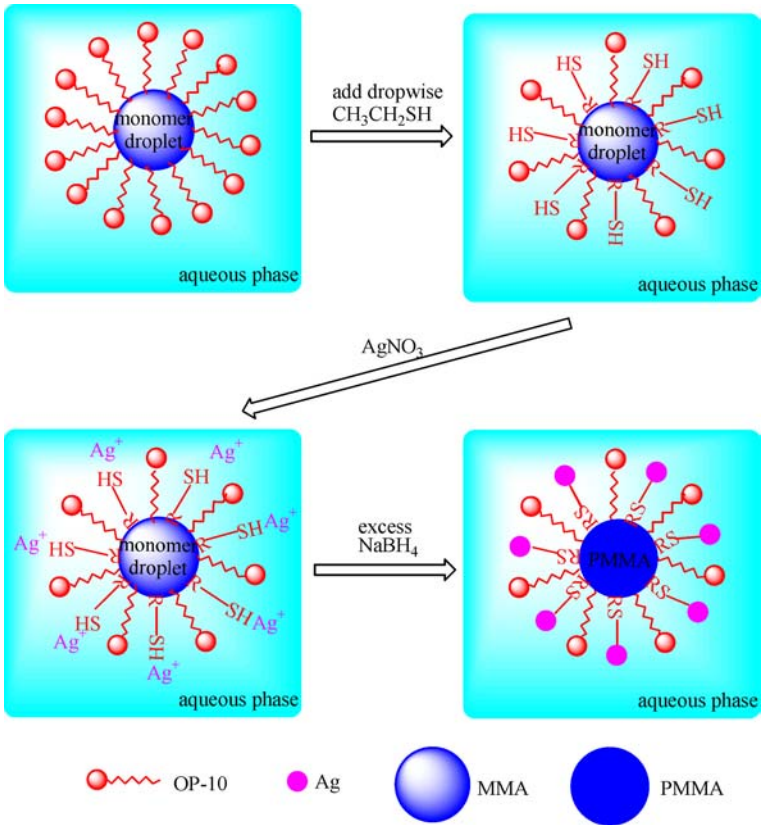

Sch. 1 The fabrication procedure of the silver-PMMA nanocomposite

was carried out. Figure 5 is the ESR spectrum of the silver-PMMA nanocomposite. There is a clean 9-line spectrum. This implies that the mechanism of polymerization is free radical in nature. The ESR spectra obtained from MMA monomers and polymers by a variety of methods have been studied over many years. The well-known 5-line (4- + 5-line) spectrum with an alternating intensity distribution and hyperfine splitting (HFS) of 11.5 G was first reported by Schneider et al., from the X-irradiation of PMMA in 1951 [21]. Later, many observations have been reported of a 9-line ESR spectrum for PMMA resulting from ^{60}Co γ-radiation [22], ultraviolet light [23], mechanical degradation [24] or ultrasound initiate [25].

In our case, there may exist two different radicals, R1 and R2, as shown in the following mechanism. In the R1 radical, the unpaired electrzons interact only with the CH_2 protons equivalently and cause HFS. In that case, a 3-line (triplet) ESR spectrum (intensity, 1:2:1, $a_H^{\alpha} = 22.4$ G) is produced as indicated in Fig. 5a. The R2 radical has two different conformations as indicated in Fig. 5b and c. The conformation indicated in Fig. 5b is most reasonably attributed to the triplet ESR spectrum of a nitrogen (identical intensity; $a_N = 16.0$ G) (the hyperfine coupling constant we got is a little larger than the previous reported data $a_N = 15.2$ G [26], likely due to the different solvent adopted). In the case of conformation indicated in Fig. 5c, two β-proton of DMPO ring interact equivalently with the unpaired electron and cause HFS. It generates a triplet ESR spectrum (intensity, 1:2:1; $a_H^{\beta} = 22.4$ G). The structure of the radical consistently follows Eqs. 1–4. The superposition of the 9-line spectrum of R2 radical and the 3-line spectrum of the polymer-propagating radicals (R1) still give the observed 9-line spectrum, because the signal intensity of the R1 radical is much smaller than that of R2.

$$2Ag^+ + BH_4^- + 3H_2O \longrightarrow 2Ag + H_2BO_3^- + 2H^+ + 3H_2 \quad (1)$$

$$BH_4^- + 3H_2O \longrightarrow H_2BO_3^- + 2H^{\bullet} + 2H^+ + 2H_2 \quad (2)$$

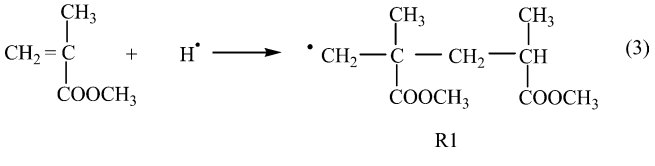

(3)

R1

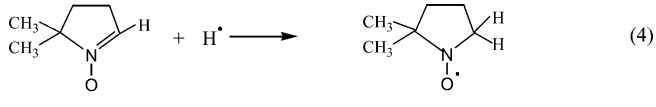

(4)

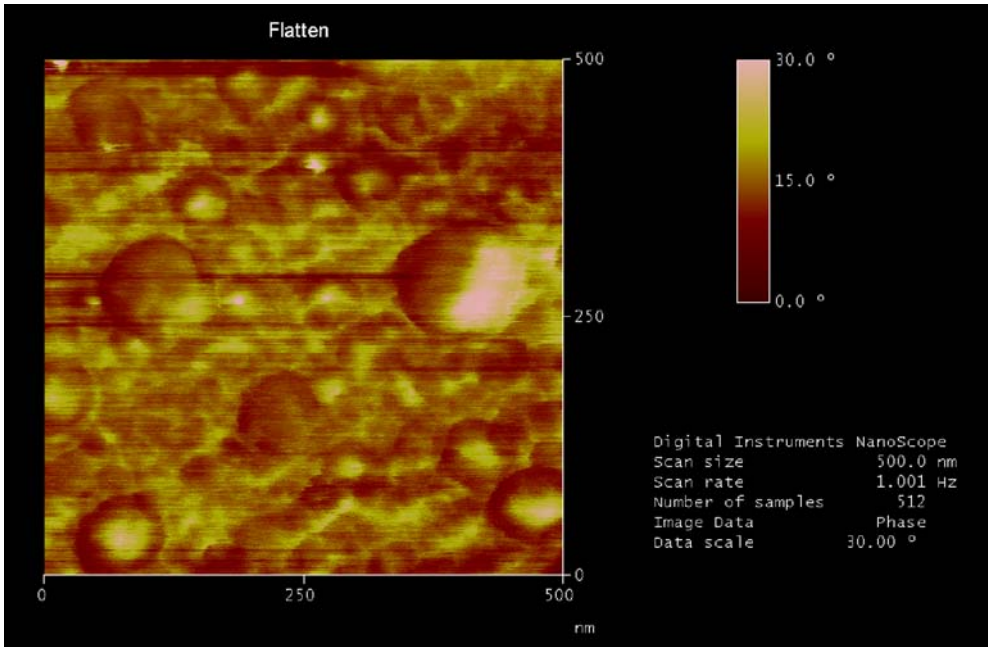

Fig. 4 Atomic force microscopy (AFM) phase-images of the silver-PMMA nanocomposite

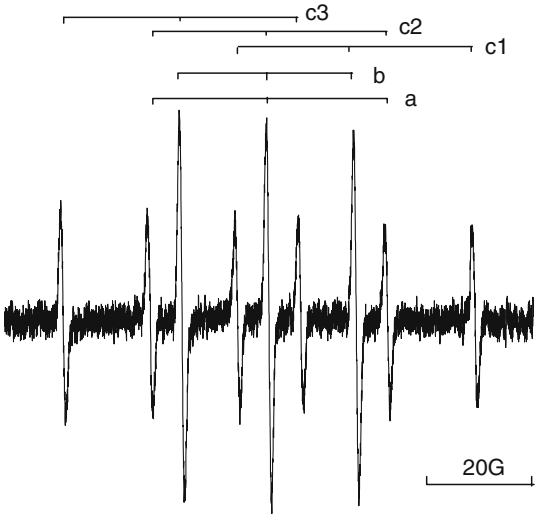

Fig. 5 electron spin resonance (ESR) spectrum of the silver-PMMA nanocomposite in air for 30 h at room temperature

In order to provide further evidence to the above mechanism, glucose and ascorbic acid have been used as reductants of silver ion instead of the $NaBH_4$. It was found that no polymer was formed.

Preparation conditions on the size of particles

Dynamic light scattering measurements were carried out to analyze the size and distribution of the particles. The influence of the preparation conditions on the size of the nanoparticle is listed in Table 1. It

Table 1 The influence of preparation conditions on the size of the nanoparticles

Sample	$AgNO_3$ (mmol/L)	$AgNO_3/CH_3CH_2SH$ (molar ratio)	Number average size (nm)	Peak width
1	30.00	6/1	70.92	19.20
2	4.30	6/1	62.39	15.91
3	4.30	1/1	50.02	12.86
4	0.43	6/1	2.46	0.66

(Note: $AgNO_3/NaBH_4$ (molar ratio) = 1:14)

can be seen that the size of the particle decreases with decreasing $AgNO_3$ concentration at given $AgNO_3/CH_3CH_2SH$ and $AgNO_3/NaBH_4$ molar ratios. When the concentration of $AgNO_3$ reduces to 10^{-1} mmol/L, the size of the particle sharply decreases to 2.46 nm. This may be because there are not enough free radicals formed by the redox system to initiate the polymerization of MMA. Therefore, the particles obtained only consist of pure silver. The molar ratio of $AgNO_3$ to mercaptoethanol also influences the size of the particle.

Conclusions

This article provides a simple fabrication method for silver-PMMA nanocomposites. Well-dispersed Ag nanoparticles are formed on the surface of PMMA nanospheres by one-pot route. The free radical mechanism of the polymerization has been verified by ESR. The average size of the nanoparticles is about 70 nm in

diameter with the shell thickness of ca. 10 nm. The size of particles decreases with decreasing $AgNO_3$ concentration at a given $AgNO_3/CH_3CH_2SH$ molar ratio. The silver nanoparticles have been widely used as the active substrates for SERS [27], chemical and optical sensors [28], and photocatalysts for solar energy conversion [29]. Therefore, further development of this kind of hybrid materials seems to be very promising.

Acknowledgements The research work is supported by the Fund of Innovation Project on Doctoral Dissertation of Donghua University.

References

1. Seeman NC (2001) Nano Lett (Communication) 1:22
2. Fendler JH, Meldrum FC (1995) Adv Mater 7:607
3. Lewis LN (1993) Chem Rev 93:2693
4. Alivisatos AP (1996) Science 271:933
5. Oldenburg SJ, Westcott SJ, Averitt RD (1999) J Chem Phys 111:4729
6. Schmidt TJ, Noeske M, Gasteiger HA (1998) J Electrochem Soc 145:925
7. Colvin VL, Schlamp MC, Alivisatos AP (1994) Nature 370:354
8. Emory SR, Nie S (1998) J Phys Chem B 102:493
9. Bruchez M Jr, Moronne M, Gin P (1998) Science 281:2013
10. Chen CW, Serizawa T, Akashi M (1999) Chem Mater 11:1381
11. Oldenburg SJ, Averitt RD, Wetcott SL, Halas NJ (1998) Chem Phys Lett 288:243
12. Ianos P, Thomas JK (1987) J Colloid Interface Sci 117:505
13. Zhang ZB, Cheng HM, Ma JM (2001) J Mater Sci Lett 20:439
14. Kobayashi Y, Salgueirino-Maceria V, Liz-Marzan LM (2001) Chem Mater 13:1630
15. Shibata S, Aoki K, Yano T, Yamane M (1998) J Sol Gel Sci Technol 11:279
16. Zhong JJ, Chun YL, Yun L (2003) Chem Lett 32:668
17. Wang LM, Chen DJ (2004) Chem Lett 8:1010
18. Dong AG, Wang YJ, Tang Y (2002) Chem Commun 4:350
19. Chen X, McGurk SL et al (1998) Macromolecules 31:2278
20. Chen CW, Chen MQ, Serizawa Takeshi, Akashi Mitsuru (1998) Adv Mater 10:1122
21. Schneider EE, Day MJ, Stein G (1951) Nature 168:645
22. Gilbro T, Kinell PO, Lund A (1971) J Polym Sci A 29:1495
23. Chen CR, Knight Randall L, Pollock Lori (1987) J Polym Sci A 25:127
24. Tatar Leyla, Kaptan HYilmaz (1997) J Polym Sci B 35:2195
25. Gu CB, Wang DJ, Wang XQ et al (2002) J Appl Polym Sci 86:1731
26. Kunitake Toyoki, Murakami Shigeru (1974) J Polym Sci Polym Chem Ed 12:67
27. Siiman O, Lepp A, Kerker M (1983) Chem Phys Lett 100:163
28. Armelao L, Bertoncello R, De Dominicis M (1997) Adv Mater 9: 736
29. Sun T, Seff K (1994) Chem Rev 94:857